

Field evolution of quantum critical and heavy Fermi-liquid components in the magnetization of the mixed valence compound β -YbAlB₄

Yosuke Matsumoto,^{1,*} K. Kuga,¹ Y. Karaki,^{1,2} Y. Shimura,¹
T. Sakakibara,¹ M. Tokunaga,¹ K. Kindo,¹ and S. Nakatsuji^{1,†}

¹*Institute for Solid State Physics, University of Tokyo, Kashiwa, Chiba 277-8581, Japan*

²*Faculty of Education, University of the Ryukyus, Nishihara, Okinawa 903-0213, Japan*

(Dated: August 19, 2021)

We present the high-precision magnetization data of the valence fluctuating heavy fermion superconductor β -YbAlB₄ in a wide temperature range from 0.02 K to 320 K spanning four orders of magnitude. We made detailed analyses of the T/B scaling of the magnetization, and firmly confirmed the unconventional zero-field quantum criticality (QC) without tuning. We examined other possible scaling relationship such as $T/(B - B_c)^\delta$ scaling, and confirmed that $\delta = 1$ provides the best quality of the fit with an upper bound on the critical magnetic field $|B_c| < 0.2$ mT. We further discuss the heavy Fermi-liquid component of the magnetization after subtracting the QC component estimated based on the T/B scaling. The temperature dependence of the heavy Fermi-liquid component is found very similar to the magnetization of the polymorph α -YbAlB₄. In addition, the heavy Fermi-liquid component is suppressed in the magnetic field above ~ 5 T as in α -YbAlB₄. This was also confirmed by the magnetization measurements up to ~ 50 T for both α - and β -YbAlB₄. Interestingly, the detailed analyses revealed that the only a part of f electrons participates in the zero-field QC and the heavy fermion behavior. We also present a temperature - magnetic field phase diagram of β -YbAlB₄ to illustrate how the characteristic temperature and field scales evolves near the QC.

PACS numbers: 71.27.+a, 71.28.+d, 74.40.Kb, 75.20.Hr, 75.30.Mb

I. INTRODUCTION

Formation of novel quantum phases in the vicinity of a quantum critical point (QCP) has been studied extensively in condensed matter physics for a past few decades. Especially, in the heavy fermion intermetallic systems, a number of prototypical examples of novel phenomena, such as unconventional superconductivity and non-Fermi liquid (NFL) behavior, have been discovered in the vicinity of a magnetic QCP where the magnetic ordering temperature is suppressed to zero¹⁻³.

So far, these studies of quantum criticality (QC) have been restricted mostly to the Kondo lattice systems with integer valence. On the other hand, the first Yb-based heavy fermion superconductor β -YbAlB₄ provides a unique example of a QC in the strongly mixed valence state⁴⁻⁷. Furthermore, the QC cannot be described by the standard theory for the spin-density-wave instability⁸⁻¹⁰. The diverging magnetic susceptibility along the c -axis exhibits T/B scaling in the wide temperature (T) and magnetic field (B) region spanning 3 \sim 4 orders of magnitude. This indicates that the QCP is located just at the zero magnetic field within the experimental resolution of 0.2 mT under ambient pressure⁶. The QC emerging without tuning any control parameter suggests a formation of an anomalous metallic phase.

β -YbAlB₄ has the locally isostructural polymorph α -YbAlB₄, which has, in contrast, a Fermi liquid (FL) ground state at zero field¹¹. α -YbAlB₄ is also strongly mixed valent. The Yb valence estimated by a hard x-ray photoemission spectroscopy is +2.73 for α -YbAlB₄ and +2.75 for β -YbAlB₄ at 20 K⁷. The valence fluctuation

temperature scale was estimated to be ~ 300 K from X-ray adsorption measurements for the both systems¹². Correspondingly, peaks have been found in the magnetic part of the in-plane resistivity (ρ_{ab}^m) and the in-plane magnetic susceptibility in the same temperature range of $200 < T < 300$ K. Nevertheless, these two systems exhibit a heavy fermion (HF) state with Kondo lattice like localized moments far below the valence fluctuation scale⁶. This is quite unusual because Pauli paramagnetism is usually expected in the mixed valence compounds below the valence fluctuation temperature scale. The small temperature scale of ~ 8 K for the anomalous HF state may indicate that α -YbAlB₄ is also close to a QCP. The origin of the HF state is a key to understand the novel QC in β -YbAlB₄, which challenges the conventional understanding of the QC based on the so called Doniach phase diagram.

Here, we discuss the magnetization (M) in β -YbAlB₄ in the T range from 0.02 K to 320 K spanning four orders of magnitude and see how it evolves with magnetic field. First, we provide a T - B phase diagram in order to overview the various T and B scales for β -YbAlB₄. Then, we present the temperature dependence of $-dM/dT$ in a wider T region between 0.02 K and 320 K than the previous report⁶. To verify the zero field quantum criticality, we examine a possibility of other scaling such as $T/(B - B_c)^\delta$ scaling with $B_c \neq 0$ or $\delta \neq 1$, and confirm that the T/B scaling reported in our previous work provides the best quality of the fitting.

We will further discuss the heavy Fermi-liquid component of M after subtracting the QC component estimated by using the T/B scaling. The obtained heavy

Fermi-liquid component exhibits the T dependence quite similar to α -YbAlB₄ having a peak in $-dM/dT$ at ~ 8 K. Recently, it has been revealed that the HF state in α -YbAlB₄ is suppressed in the magnetic field above ~ 5 T¹³. Here we found that the heavy Fermi-liquid component of M in β -YbAlB₄ also exhibits a field evolution quite similar to the one for α -YbAlB₄, suggesting that the HF state in β -YbAlB₄ is also suppressed in the magnetic field above ~ 5 T. This was also confirmed by the measurements of the magnetization curve up to ~ 50 T for both α - and β -YbAlB₄. In addition, it further indicates that only a part of f electrons participates in the zero-field QC and exhibits the HF behavior.

Note that partial results presented here have already been discussed in Refs.^{6,14,15}. The experimental details of this work can be found in Refs.^{6,14}. We also note that M was measured with the resolution of $\sim 10^{-8}$ emu by the high precision SQUID magnetometer installed in a ³He-⁴He dilution refrigerator at $T < 4$ K and $B < 0.05$ T. The residual magnetic field was as small as ~ 1.1 μ T. At $T < 4$ K and $B \geq 0.05$ T, it was measured with a resolution of $\sim 10^{-5}$ emu by a high precision Faraday magnetometer installed in a ³He-⁴He dilution refrigerator¹⁶. We employed only high quality single crystals after carefully washed the surface of each crystal to remove possible impurities. The residual resistivity ratio (RRR) of the samples used for the SQUID magnetometer measurements (~ 30 pieces, 0.82 mg) was higher than 200. For the Faraday magnetometer measurements, we used single crystals of 7.5 mg, whose typical RRR is as high as 140. The higher T measurements above 2 K were done by a commercial SQUID magnetometer. High field magnetization curves up to ~ 50 T were measured using a pulsed field facility at the ISSP of the University of Tokyo. Both of these two sets of measurements were done for both β -YbAlB₄ and α -YbAlB₄ for the samples with typical RRR of 140 and 50, respectively.

II. RESULTS AND DISCUSSION

A. T - B phase diagram

In order to overview the characteristic T and B scales in β -YbAlB₄, we first present a T - B phase diagram for the field applied along the c -axis in Fig. 1. To construct the phase diagram, we used all the data available so far including those we will present and discuss later in this paper.

Let us begin with the high T region of the phase diagram. A pink arrow at $T \sim 290$ K indicates the valence fluctuation scale estimated by the X-ray adsorption measurements¹². The coherence peak observed in the in-plane resistivity ρ_{ab} at $T \sim 270$ K (red arrow) and a peak in χ_{ab} found at $T \sim 210$ K for $B = 0.1, 7.0$ T (dark yellow arrow) also correspond to the valence fluctuation scale. On cooling, another scale ~ 50 K emerges as the effective Kondo temperature for the low T HF behavior.

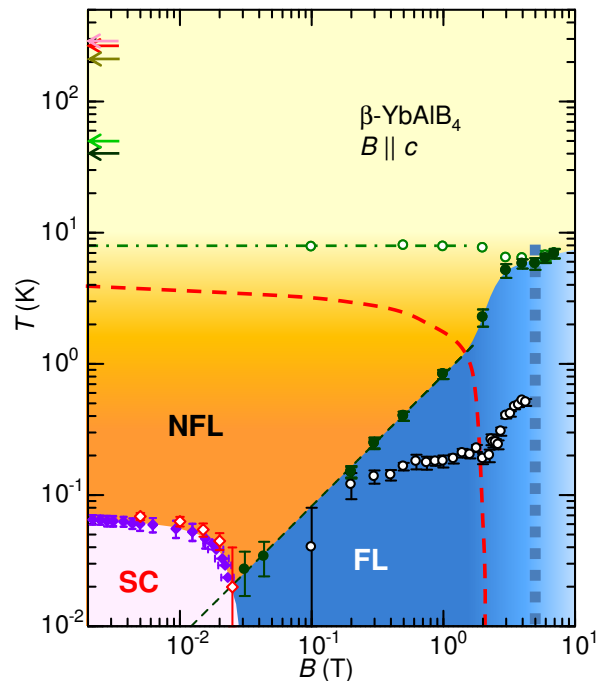


FIG. 1: T - B phase diagram of β -YbAlB₄ for the field applied along the c -axis. The valence fluctuation scale is shown as pink, red and dark yellow arrows at $T \sim 200 - 300$ K which corresponds to T scale obtained by X-ray adsorption¹², the coherence peak in ρ_{ab} ⁴ and a peak in χ_{ab} at $B = 0.1, 7.0$ T, respectively. The light and dark green arrow indicate the anomaly in the T derivative of the in-plane resistivity $d\rho_{ab}/dT$ at $T \sim 50$ K¹¹ and the peak in the Hall coefficient R_H at ~ 40 K¹⁷, respectively. These temperature scales correspond to the effective Kondo lattice temperature for the low T HF behavior. Green filled circles correspond to the peaks in $d\chi/dT$, which separates the QC and FL regions. Green open circles correspond to the peak temperature scale T^* in $\Delta(-d\chi/dT)$ obtained after subtracting QC components, which sets the onset of the heavy fermion state. Black open circles correspond to T_{FL} determined by ρ_{ab} ⁴. Filled and open diamonds correspond to superconducting phase boundary determined by the SQUID ac susceptibility measurements¹⁴ and the resistivity measurements⁵, respectively. Inside the red broken line, the QC scaling is observed. The vertical blue broken line at $B \sim 5$ T indicates the crossover field above which the HF state is suppressed. For detail, see text.

For example, M starts to increase below $T \sim 40$ K signaling the onset of the HF behavior, as we will discuss. At the same T -range, the Hall coefficient R_H exhibits a pronounced peak indicating a coherence developing among f electrons¹⁷. In addition, the T derivative of the in-plane resistivity $d\rho_{ab}/dT$ shows a shoulder-like anomaly at $T \sim 50$ K¹¹.

Far below the valence fluctuation scale, we find another T scale for the HF behavior at $T^* \sim 8$ K, typically in the susceptibility $\chi = M/B$ along the c -axis. As we will discuss later in detail, $\chi(T)$ along the c -axis consists of two components, *i.e.*, the QC and the heavy

Fermi-liquid components. T^* is defined as a peak temperature of the heavy Fermi-liquid component of $-d\chi/dT$ in β -YbAlB₄ which is represented by $\Delta(-d\chi/dT)$. For α -YbAlB₄, T^* denotes the peak in $-d\chi/dT$. Below T^* , β -YbAlB₄ indicates the unconventional zero-field QC, while α -YbAlB₄ exhibits the FL properties at $B = 0$.

The T/B scaling of M was observed in the regime below $B \leq 2$ T and $T \leq 3$ -4 K which is a region inside the red dashed line in Fig. 1. Inside the region, the QC component exceeds the heavy Fermi-liquid component. The NFL-FL crossover is defined by the peak in $-dM/dT$ (or $-d\chi/dT$) and is observed on the line where $T/B \sim 0.8$ K/T. This linear field dependence of the peak corresponds to the Zeeman energy scale of an effective moment $\sim 1.94 \mu_B$ ^{6,14}. The peak in $-dM/dT$ merges into the one for $\Delta(-d\chi/dT)$ at $B \geq 2$ T where the heavy Fermi-liquid component is dominant. The zero-field QCP is masked by the HF superconductivity observed at $T \leq 0.08$ K and $B \leq 0.03$ T along the c -axis. Note that the small T_c enables us to reveal the zero-field QC behaviors in detail. ρ_{ab} exhibits T^2 behavior below T_{FL} which is much lower than the NFL-FL crossover temperatures. The HF behavior is suppressed above $B^* \sim 5$ T, a characteristic field scale determined by M (the vertical thick dashed line in dark blue in Fig. 1). T_{FL} shows a sudden increase at 2.3 T suggesting the suppression of the HF behavior at a slightly smaller field than $B^* \sim 5$ T. We will further discuss this in detail later.

Thus, both β -YbAlB₄ and α -YbAlB₄ have the three contrasting temperature scales, *i.e.*, the valence fluctuation scale of 200 - 300 K, the effective Kondo temperature ~ 50 K, and the HF T scale of $T^* \sim 8$ K.

B. Overview of the magnetization data

Next, we discuss the magnetization (M) data measured over four decades of T (0.02 K to 320 K) and B (0.3 mT to 7 T) in detail. The divergent susceptibility $\chi = M/B$ along the c -axis is one of the most remarkable features of the QC in β -YbAlB₄⁶. In order to discuss the divergent behavior of χ as a function of T and B , we show $-dM/dT$ versus T for selected fields along the c -axis on a logarithmic scale in Fig. 2 for both α - and β -YbAlB₄. As is clearly seen in the figure, below $T \sim 3$ K, $-dM/dT$ for the β phase shows a power law behavior with $T^{-1.5}$ dependence (broken line), indicating the divergence of the susceptibility $\chi \sim T^{-1/2}$ in the non-Fermi liquid region at $T/B \gtrsim 1$ K/T. On the other hand, a T -linear behavior (solid line) is observed at $T/B \lesssim 1$ K/T, which is expected for a FL state. By applying magnetic field, the quantum critical component is suppressed and finally masked by another component which appears at $T^* \sim 8$ K. At $B = 7.0$ T, it overlaps on top of the one for α -YbAlB₄ at least down to $T \sim 2$ K. This crossover at $T^* \sim 8$ K is commonly seen in both β - and α -YbAlB₄ and gives characteristic T -scale of the Kondo lattice behavior. The low T magnetization of β -YbAlB₄ is well ex-

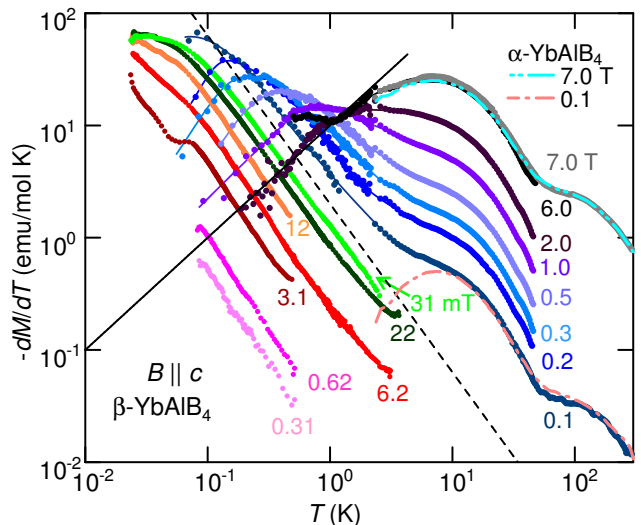


FIG. 2: $-dM/dT$ versus T for selected fields along the c -axis on a logarithmic scale for both β - (solid circles) and α -YbAlB₄ (long dashed dotted line for $B = 0.1$ T and long dashed double-dotted line for $B = 7.0$ T). The sudden downturn below 0.1 K in the low field data corresponds to the onset of superconductivity.

pressed by a sum of the QC component $M_c/B \propto T^{-0.5}$ and T -independent constant term $\chi_0 (= M_0/B) = 0.017$ (emu/mol) which is close to the zero- T susceptibility of the non-critical α -YbAlB₄ and may originate from a constant Van Vleck component to the susceptibility and/or from Pauli susceptibility of the non-critical parts of the Fermi surfaces. This heavy Fermi-liquid component is extracted after subtracting the QC component. We will further discuss the detail of this component later.

C. T/B scaling and the evaluation of its quality

As we already reported in the previous paper⁶, if we plot $(-dM/dT)B^{0.5}$ vs. T/B for β -YbAlB₄, all the data in the region of $T \lesssim 3$ K and $B \lesssim 2$ T enclosed by the red broken line in Fig. 1 collapse on a single curve (Fig. 3 (a)). This indicates a scaling relation of

$$-\frac{dM}{dT} = B^{\alpha-2} \phi\left(\frac{T}{B}\right), \quad (1)$$

with $\alpha = 3/2$. The reason why we use $-dM/dT$ rather than $M_c = M - M_0$ is that $-dM/dT$ is free from the ambiguity in the estimate of χ_0 and its field evolution. In fact, the scaling obtained for $-dM/dT$ looks better than that of M_c , *i.e.*, $M_c/B^{0.5}$ vs. T/B ^{6,18}. This empirical scaling relation implies that close to the QCP, β -YbAlB₄ has no intrinsic energy scale and the ratio T/B determines the physical properties. The peak of the scaling curve is located at $T/B \sim 0.8$ K/T, defining the thermodynamic boundary between the FL and NFL regions

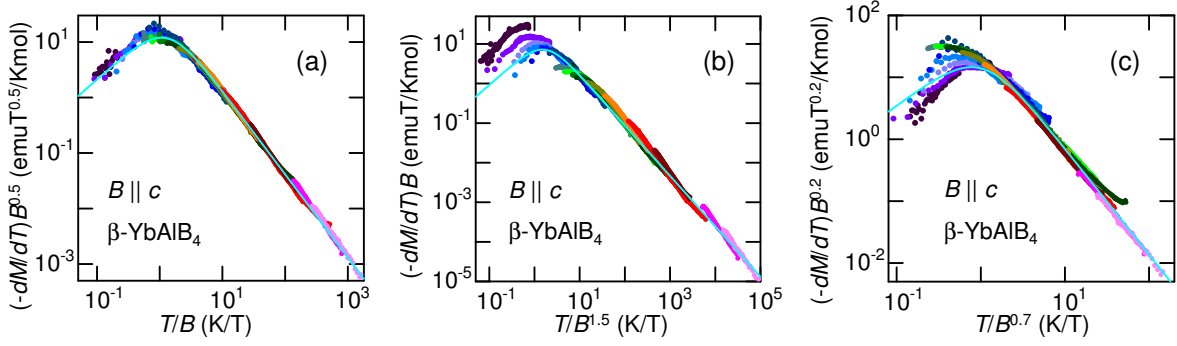


FIG. 3: Scaling plots $(-dM/dT)B^\eta$ vs T/B^δ with (a) $(\delta, \eta) = (1.0, 0.5)$, (b) $(\delta, \eta) = (1.5, 1.0)$, (c) $(\delta, \eta) = (0.7, 0.2)$ for the data shown in Figure 2(a) inset. The light blue lines are the fit by $\phi(x) = \Lambda x(A + x^2)^{\frac{\alpha}{2}-2}$ (see text).

in the T - B phase diagram (Fig. 1). As already discussed in the previous report⁶, the scaling behavior can be well fitted to Eq. (1) with

$$\phi(x) = \Lambda x(A + x^2)^{\frac{\alpha}{2}-2}, \quad (2)$$

for $\alpha = 3/2$. This form was chosen to satisfy the limiting behaviors of the QC free energy $F_{\text{QC}} = B^\alpha f(T/B)$ obtained after integrating the both parts of Eq. (1). Here $f(x)$ is related to $\phi(x)$ by $\phi(x) = (\alpha - 1)f'(x) - xf''(x)$. Indeed, this satisfies $f(x) \propto x^\alpha$ in the NFL regime ($x \gg 1$) and $f(x) \propto \text{const} + x^2$ in the FL phase ($x \ll 1$).

The T/B scaling implies that the critical field B_c of the quantum phase transition is located just at zero field because a finite value of B_c requires the scaling function $\phi(x)$ with a ratio $x = T/|B - B_c|$ rather than $x = T/B$. In the previous work, B_c , which gives the best fitting of the experimental data to Eq. (1), was estimated to be -0.1 ± 0.1 mT by using Eq. (2). This is comparable to the Earth's magnetic field (~ 0.05 mT) and two orders of magnitude smaller than $\mu_0 H_{c2} = 30$ mT. This tiny value indicates zero-field quantum criticality without tuning in β -YbAlB₄⁶.

If we take into account a possibility of other scaling, such as T/B^δ scaling with $\delta \neq 1$ and a possibility of finite B_c , the scaling relation in Eq. (1) will be generalized as follows.

$$-\frac{dM}{dT} = (B - B_c)^{-\eta} \phi\left(\frac{T}{(B - B_c)^\delta}\right). \quad (3)$$

The qualitative evaluation of these possible scaling relations can be made by plotting $(-dM/dT)(B - B_c)^\eta$ versus $T/(B - B_c)^\delta$ for the same data set for the region shown in Fig. 2(a) inset while changing B_c , δ and η . The examples of the other plots with $(B_c, \delta, \eta) = (0, 1.5, 1.0)$ and $(0, 0.7, 0.2)$ are shown in Fig. 3 (b) and (c) respectively. Compared to the scaling plot in Fig. 3 (a), the data in these two examples do not collapse on a single curve.

In order to quantitatively evaluate the quality of the scaling, here we use the correlation R obtained after fitting $\phi(x)$ with $x = T/(B - B_c)^\delta$ to the data for each set of

the parameters. Here R is defined as $R \equiv \sqrt{1 - \chi^2/\text{DOF}}$ where χ^2 is a statistical one and DOF (degree of freedom) is a number of the data points (2227 points). R takes its maximum value of 1 if the fitting quality is perfect. In order to obtain a reasonable fit in a log-log scale, we fit the data with the weight of $(1/\sigma_i)^2 = (-dM_i/dT)(B - B_c)^\eta)^2$ for i -th data. Otherwise, the power law behavior observed at the large x region cannot be fitted well due to its small value. We checked a parameter region of $-0.5 \text{ mT} \leq B_c \leq 0.2 \text{ mT}$, $0.5 \leq \delta \leq 1.5$, $0.1 \leq \eta \leq 1.0$ with interval of 0.1 mT, 0.1 and 0.1, respectively. In addition, fittings with more fine grid were done at a parameter region of $-0.2 \text{ mT} \leq B_c \leq 0.2 \text{ mT}$, $0.86 \leq \delta \leq 1.10$, $0.30 \leq \eta \leq 0.66$ with interval of 0.02 mT, 0.02 and 0.02, respectively. We created scaling plots of totally $\sim 1.2 \times 10^4$ combinations of parameters. Each of them was fitted to Eq. (2) and the correlation R was evaluated. Here Λ , A and α are free fitting parameters.

The best fit with the maximum value of $R = 0.996$ is obtained at $(B_c, \delta, \eta) = (-0.02 \pm 0.20 \text{ mT}, 0.94 \pm 0.12, 0.46 \pm 0.12)$. This result is consistent with $(0, 1.0, 0.5)$ proposed originally in Ref.⁶, and further indicates that the data in the widest T and B range are scaled with this parameter set. The errors for the parameters B_c , δ and η were determined by the parameter space where $R \gtrsim 0.993$. Here we assumed that the error in R is given by the difference between the maximum $R = 0.996$ and the ideal value of 1. The contour plot of R is shown in Fig. 4. Here, η was chosen for each set of fixed B_c and δ so that it gives maximum R . An example at $B_c = 0$ is shown in the inset of Fig. 4. This corresponds to adjusting η against δ under fixed B_c so that a scaling is realized at high T parts where the NFL power-law behavior is observed. The fitting results to the plots with $(B_c, \delta, \eta) = (0, 1.5, 1.0)$ and $(0, 0.7, 0.2)$ are shown in Figs. 3 (b) and (c) by the solid lines. These parameter sets are located at the top and bottom of the vertical broken line of $B_c = 0$ in Fig. 4 where $R = 0.956, 0.969$, respectively. As is clearly seen in Fig. 4, no other scaling is possible with the parameter set away from $(B_c, \delta, \eta) = (0, 1.0, 0.5)$.

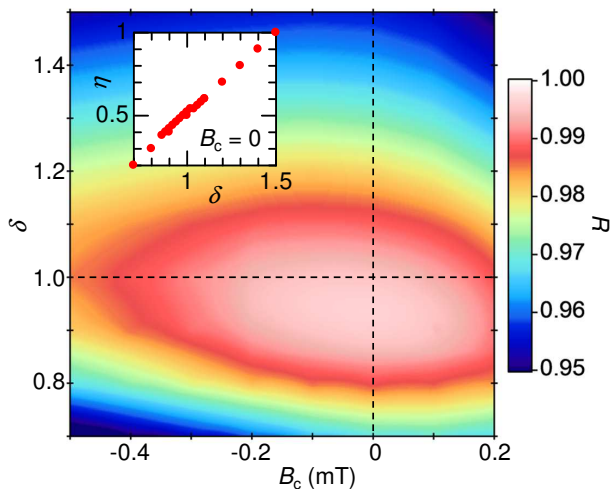


FIG. 4: Contour plot of the correlation R obtained from the fitting $\phi(x)$, where $x = T/(B - B_c)^\delta$, to the scaling plot (see text). Here, η is chosen for each δ with fixed B_c so that each η gives maximum R as shown in the inset as an example at $B_c = 0$.

From the above discussion, we confirm that the scaling law reported in Ref.⁶ provides the best fitting quality. This sets an important bound for theoretical explanation of the QC behavior found in β -YbAlB₄. First of all, this type of scaling behavior cannot be explained by the standard theory based on spin-density-wave type fluctuations⁶. On the other hand, a recent study of the Anderson impurity model demonstrates that Kondo destruction at a mixed valent QCP is possible and indeed the T/B scaling (and ω/T scaling) is reproduced around the QCP¹⁹. It is an interesting future issue whether this is still relevant even in the lattice limit.

Another interesting possibility has been discussed based on the anisotropy in the hybridization between the conduction and f electrons (c - f hybridization)²⁰. From the argument based on the local symmetry of the Yb site, the crystal field ground doublet of both α -YbAlB₄ and β -YbAlB₄ is suggested to be made solely of $|J_z = \pm 5/2\rangle$ ²¹. In this case, the c - f hybridization is expected to be highly anisotropic as it has been already suggested experimentally for α -YbAlB₄¹¹ and have a node along the c -axis. The theory proposes that this results in a heavy flat band with a k^4 dispersion and the QC in β -YbAlB₄ can be understood as a novel type of topological Fermi surface instability that should arise when the f level is tuned to the bottom of the band. Interestingly, the theory reproduces the observed T/B scaling in M quite well. However, in this scenario, a pinning mechanism of the f level to the bottom of the band remains as an open question. In order to examine the relevance of this theory, further studies, especially on the detail of the Fermi surface, are required.

The effect of the critical valence fluctuations associated with a valence QCP or valence crossover²² might be

also the key to understand the unconventional QCP in β -YbAlB₄. Interestingly, a recent theory has demonstrated the robustness of the valence QCP against pressure to explain the QC found in an Yb-based quasicrystal^{23,24}. Furthermore, it is worth noting that the theory reproduces the T/B scaling especially at the NFL regime where $T/B \geq 0.8$ K/T²⁵. Measurements of the dynamical valence susceptibility will be the key to clarify whether the valence fluctuations are the origin of the observed QC behaviors.

In any case, there are apparently a lot of experimental and theoretical works to be done in order to understand the origin of the QC in β -YbAlB₄. Among them, the mechanism of the HF formation even in the strong valence fluctuation may be the most fundamental problem to be answered. In the following, in order to give more insight into the HF behavior, we will discuss the details of the heavy Fermi-liquid component of M obtained after subtracting the QC component, in particular focusing on its magnetic field evolution and the corresponding suppression of the HF behavior.

D. Heavy Fermi-liquid component of the magnetization

As already discussed above, while the QC component is suppressed by applying B , there is another component peaking at $T^* \sim 8$ K in $-dM/dT$. This becomes dominant with increasing B and finally overlaps on top of the one for α -YbAlB₄ at $B = 7.0$ T (Fig. 2 (b)). In order to discuss the field evolution of this heavy Fermi-liquid component in detail, we subtracted the QC component at each B by using the obtained scaling equation with the fitting parameters $(B_c, \delta, \eta) = (0, 1.5, 1.0)$ shown in Fig. 3 (a). The obtained heavy Fermi-liquid component divided by B , *i.e.*, $\Delta(-dM/dT)/B = \Delta(-d\chi/dT)$ is shown in Fig. 5. Here $-d\chi/dT$ of α -YbAlB₄, where no subtraction is made, is also shown for comparison. Interestingly, the heavy Fermi-liquid component in β -YbAlB₄ is quite similar to $-d\chi/dT$ in α -YbAlB₄ even at a low field of $B = 0.1$ T. This indicates that the magnetization of β -YbAlB₄ can be divided into two parts, the QC and the heavy Fermi-liquid components, the latter of which is similar to the one in α -YbAlB₄.

After peaking at $T^* \sim 8$ K, $\Delta(-d\chi/dT)$ exhibits a T^{-2} power law behavior on heating up to 50 K (broken line in Fig. 5), consistent with the Curie-Weiss behavior of paramagnetic local moments surviving above $T^* \sim 8$ K in both compounds. The Curie-Weiss fit to the T -linear inverse susceptibility at a somewhat lower T range extending even below $T^* \sim 8$ K ($6 \lesssim T \lesssim 15$ K) gives antiferromagnetic Weiss temperatures $\Theta_W = 29, 25$ K and Ising moments $I_z = 1.4, 1.3 \mu_B$ for the α and β phases, respectively^{6,15}. On the other hand, if we fit the asymptotic T^{-2} power law behavior at $20 \leq T \leq 50$ K to the temperature derivative of the Curie-Weiss law, we obtain $\Theta_W = 4 \pm 1, 2 \pm 1$ K for the α and β phases,

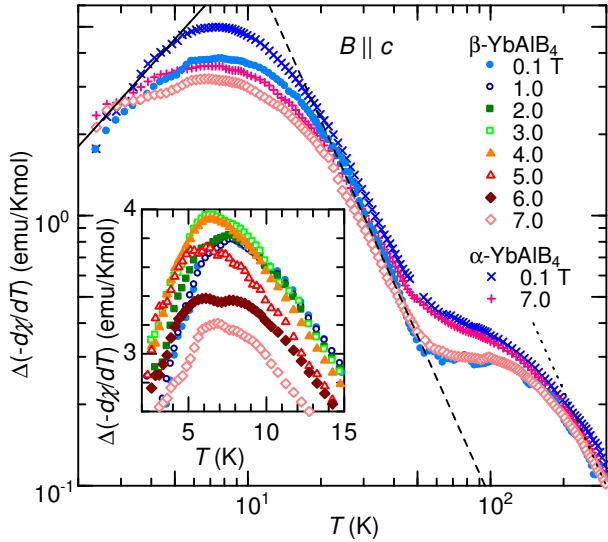


FIG. 5: Heavy Fermi-liquid component in $-d\chi/dT$ of β -YbAlB₄: $\Delta(-d\chi/dT)$ under the fields of 0.1 T and 7 T along the c -axis in the full logarithmic scale. Here, the QC component shown in Fig. 3 (a) is subtracted. $-d\chi/dT$ of α -YbAlB₄ under the same fields (where no subtraction has been made) are also shown for comparison. The solid line is the guide to the eye which represents the T -linear behavior expected for a FL phase. The broken and dotted lines are also the guides to the eye which represent T^{-2} dependence of the Curie(-Weiss) behavior in the high temperature limit (see text). Inset shows the field dependence of the peak found at $T \sim 8$ K for β -YbAlB₄ in a linear scale.

respectively, and $I_z = 0.6 \pm 0.1 \mu_B$ for both phases. The latter evaluations could be more reliable in the sense that it is free from the constant term χ_0 that has rather large error. If we adopt the latter moment sizes, the Wilson ratio becomes as high as 120 for both compounds. On the other hand, the low- T part of the peak at $T^* \sim 8$ K exhibits a T -linear behavior (solid line in Fig. 5) which is consistent with the FL ground state. Note that this is not clear for β -YbAlB₄ in the lower B below ~ 3 T due to the QC component.

Another T^{-2} power law behavior found at a high T range above 200 K corresponds to the high T Curie-Weiss behavior reported previously, which gives antiferromagnetic $\Theta_W = 110 \pm 2$, 108 ± 5 K and Ising moments $I_z = 2.22$, $2.24 \mu_B$ for α and β phases respectively^{6,15}. This crosses over to the low T Curie-Weiss behavior across $T \sim 50$ K where the T dependence of $\Delta(-d\chi/dT)$ of β -YbAlB₄ and $-d\chi/dT$ of α -YbAlB₄ indicate inflection points. Below this temperature, M in both compounds exhibits further increase on cooling, which can be regarded as the onset of the HF behavior. Note that the T derivative of the in-plane resistivity, $d\rho_{ab}/dT$, indicates a shoulder-like anomaly at $T \sim 50$ K¹¹. Furthermore, recent Hall effect measurements revealed a large peak in the T dependence of R_H at ~ 40 K. Both suggest coherence developing among f electrons¹⁷.

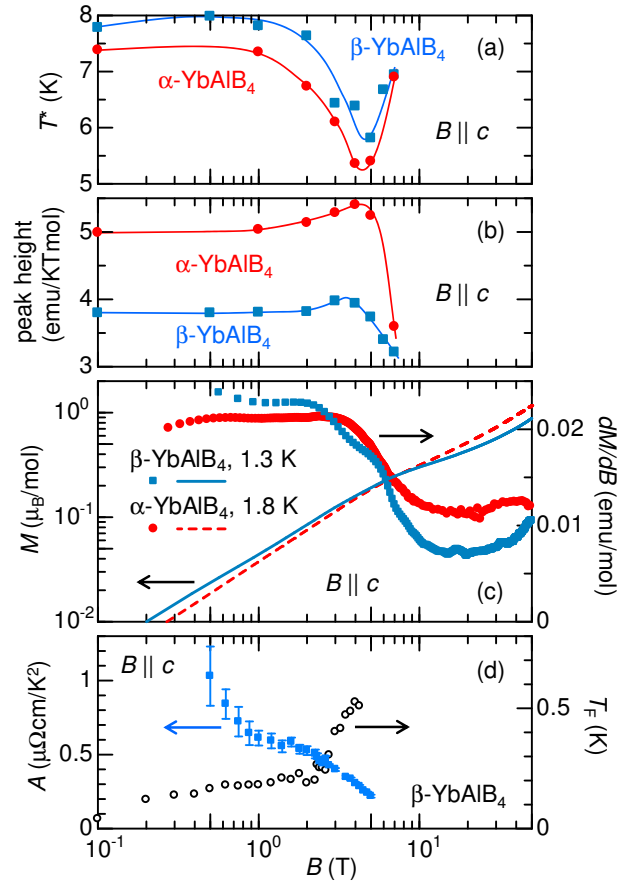


FIG. 6: Field dependence of (a) the peak temperature T^* and (b) its height for $\Delta(-d\chi/dT)$ of β -YbAlB₄ and $-d\chi/dT$ of α -YbAlB₄, respectively. (c) Magnetization curves (the left axis) and its field derivative dM/dB (the right axis) in α - and β -YbAlB₄ at $T = 1.8$ and 1.3 K, respectively. (d) Field dependence of the A coefficient and T_F determined by the in-plane resistivity ρ_{ab} of β -YbAlB₄⁴. The field is along the c -axis for all the figures. For details, see text.

E. Suppression of the heavy fermion in B

Next, we discuss the field evolution of the HF behavior in detail. As shown in the inset of Fig. 5, $\Delta(-d\chi/dT)$ in β -YbAlB₄ changes its peak height and peak temperature T^* with magnetic fields. The peak height slightly increases with field and maximizes at $B \sim 3 - 4$ T and decreases rather steeply above this field. On the other hand, T^* decreases by 30% and shows the minimum at $B \sim 4 - 5$ T. Figures 6 (a) and (b) plot the B dependence of T^* and the peak height of both $\Delta(-d\chi/dT)$ in β -YbAlB₄ and $-d\chi/dT$ in α -YbAlB₄, respectively. As clearly seen in the figure, their field evolutions are quite similar to each other except that T^* in β -YbAlB₄ is larger by several % than the one in α -YbAlB₄ and the peak height for β -YbAlB₄ is 30% smaller than for α -YbAlB₄. These field evolutions indicate a characteristic field scale of $B^* \sim 5$ T. Correspondingly, the magnetization curves

for both compounds exhibit a slope change at B^* (Fig. 6 (c)).

This field evolution can be regarded as the results of suppression of the HF behavior above $B^* \sim 5$ T, as it was already discussed for α -YbAlB₄¹³. Furthermore, in the case of α -YbAlB₄, it was discussed that the low T part of the peak in $-d\chi/dT$, at least down to 2 K, deviates from FL behavior indicating a possible NFL behavior in the lower T ¹³. Indeed, the recent transport and thermodynamic measurements down to very low temperatures below 0.1 K revealed an anisotropic NFL behavior which will be discussed elsewhere²⁶. However, in β -YbAlB₄, it is unlikely to have such a field induced NFL state at $B \sim 3 - 5$ T in addition to the one found at zero-field. There has been no indication of NFL behavior in the measurements such as the in-plane resistivity ρ_{ab} down to 40 - 50 mK⁴ and specific heat at least down to $T = 0.4$ K^{4,6}. Furthermore, $-d\chi/dT$ at $B = 3.0, 4.0$ T do not indicate clear NFL behavior (not shown). They well overlap to the one at 2.0 T indicating T -linear dependence consistent with FL (Fig. 2(b)).

The suppression of the HF behavior is also observed in the temperature dependence of ρ_{ab} . We present the B dependence of T_{FL} and A coefficient determined by ρ_{ab} in the previous work⁴ in Fig. 6 (d). Here, T_{FL} is defined as a temperature below which the resistivity exhibits the T^2 dependence. A is the coefficient for the T^2 dependence, *i.e.*, $\rho_{ab} = \rho_{ab,0} + AT^2$ where $\rho_{ab,0}$ is the in-plane residual resistivity. As already mentioned above, T_{FL} and A are well-defined for all the field above 0.1 T suggesting that there is no field induced QC. On the other hand, both T_{FL} and A indicate anomalies at $B \sim 2.3$ T which is somewhat smaller than the characteristic field scale of $B^* \sim 5$ T found in M . While T_{FL} suddenly increases above that field, A decreases making a shoulder like feature at the same field. Both of these observations indicate suppression of the HF state. Note that the further increase of A in the lower B below 1 T corresponds to the zero field QC⁴.

In general, the HF behavior is expected to be suppressed when the Zeeman energy exceeds the Kondo coupling under magnetic fields. This is sometimes accompanied by a sudden localization of f electrons (Kondo breakdown) or Lifshitz transition as suggested both experimentally and theoretically²⁷. In the case of α - and β -YbAlB₄, the suppression of the HF behavior at $B^* \sim 5$ T is supposed to reflect the renormalized small Kondo scale. If we assume that the Zeeman energy of the effective moment $g\mu_B$ becomes comparable with the Kondo scale given by $k_B T^*$ at B^* , we obtain $g\mu_B \sim 2.3 \mu_B$ by using $T^* = 7.8$ K for β -YbAlB₄ at $B = 0.1$ T. Interestingly, this is close to the value estimated from the T/B scaling and its free energy, $1.94 \mu_B$ ⁶. For α -YbAlB₄, a similar value of $g\mu_B \sim 2.2 \mu_B$ is obtained from $T^* = 7.4$ K at $B = 0.1$ T and $B^* = 5$ T.

Naively speaking, one would expect that a considerable amount of f moments become polarized if a HF state is suppressed under magnetic field. However, in α - and β -

YbAlB₄, M only reaches $\sim 0.2 \mu_B$ at B^* (Fig. 6 (c)) which is considerably smaller than the above estimation. This may indicate that only a fraction of f moments participates in the HF behavior or QC. Interestingly, the recent Hall effect measurements in β -YbAlB₄ revealed that there are two bands having different Kondo temperatures T_K , namely, a hole like band with the coherence T scale of 200 K and an electron like band with low carrier density ($\sim 10\%$) with the low T_K of ~ 40 K. Indeed, this indicates that only the latter component is responsible for the HF behavior and QC in β -YbAlB₄¹⁷. The effective moment of $0.6 \mu_B$ estimated from the low T Curie-Weiss behavior corresponds to 30% of the high T value, suggesting again that only a fraction contributes to the HF and QC components.

The suppression of the HF behavior with the similar anomaly in the magnetization curve has been observed in YbRh₂Si₂ at $B \sim 10$ T²⁸. Interestingly, while thermodynamic measurements²⁸⁻³⁰ and the de Haas-van Alphen measurements³¹ indicate only one characteristic field, recent thermal and electrical transport measurements have revealed that it consists of three successive Lifshitz transitions which interplay with a smooth suppression of the Kondo effect³². This may be also the case in β -YbAlB₄ where we found two slightly different field scales, ~ 2.3 and ~ 5 T, in ρ_{ab} and M , respectively. Further experimental studies, especially on thermal transport, will be important to clarify the origin of the multiple field scales. Note that, in YbRh₂Si₂, M at the suppression field ~ 10 T amounts to $\sim 1.1 \mu_B$. This is close to the value of $1.4 \mu_B$ estimated from low T Curie-Weiss behavior³³ indicating that the major part of the f -electrons becomes polarized. This is clearly different from our observations made in α - and β -YbAlB₄.

We have not yet clarified the mechanism of the unusual HF formation under the strong valence fluctuations. However, the fact that only a fraction of f moments participates in the HF behavior at least gives us a hint that the multiple bands and/or their topological feature may play an important role. Indeed, the two distinct T scales observed in both compounds may be ascribable to the two Fermi surfaces having different Kondo temperatures due to the anisotropic c - f hybridization. In this sense, studies on Fermiology are important future issues. On the other hand, it is an interesting and challenging future issues to check and detect the strong valence fluctuation effect such as anomalous charge fluctuations associated with the valence criticality.

III. CONCLUSION

We discussed the detailed evolution of the magnetization (M) in β -YbAlB₄ with temperature and magnetic field. We presented the temperature dependence of $-dM/dT$ obtained over a four decades of T range between 0.02 K and 320 K, which is wider than the previous report⁶. First, we checked the T/B scaling found

at the low T and the low B region in detail. In particular, we examined the possibility of other scaling such as $T/(B - B_c)^\delta$ scaling with $B_c \neq 0$ or $\delta \neq 1$, and confirmed that the T/B scaling yields the best quality for the fitting.

We further estimated the heavy Fermi-liquid component of M after subtracting the QC component by using the T/B scaling. The obtained heavy Fermi-liquid component exhibits the T and B dependence quite similar to the magnetization of α -YbAlB₄, having a peak in $-dM/dT$ at $T^* \sim 8$ K which is suppressed above $B^* \sim 5$ T. This indicates that the HF behavior in α - and β -YbAlB₄ becomes suppressed above this field corresponding to a small renormalized Kondo scale. This suppression of the HF behavior may be related to the recent observation of the field induced anisotropic NFL behavior in α -YbAlB₄²⁶. In β -YbAlB₄, on the other hand, we found no sign of such field induced NFL behavior. We note that it is an interesting question whether and how the two components found in the intermediate valence material are related to the two-fluid description of the Kondo lattice³⁴.

While the effective g -factor estimated from the Zeeman coupling relation $k_B T^* = g \mu_B B^*$ and T/B scaling suggests the effective moment of $\sim 2 \mu_B$ for β -YbAlB₄, M at the suppression field B^* only reaches a considerably smaller value $\sim 0.2 \mu_B$. This indicates that only a part of the f moments participates in the zero-field QC or HF behavior, as also suggested by the recent Hall effect measurements¹⁷. The multiple bands and their topological feature should play an important role in the formation of the low temperature heavy fermion state and quantum criticality in the intermediate valence state.

Acknowledgments

We thank E. C. T. O'Farrell, P. Coleman, A. H. Nevidomskyy, S. Watanabe, C. Broholm, K. Ueda for supports and useful discussions. This work is partially supported by Grants-in-Aid (No. 21684019) from JSPS, by Grants-in-Aids for Scientific Research on Innovative Areas (No. 20102007, No. 21102507) from MEXT, Japan.

-
- * matsumoto@issp.u-toyko.ac.jp
 † satoru@issp.u-tokyo.ac.jp
- ¹ N. D. Mathur, F. M. Grosche, S. R. Julian, I. R. Walker, D. M. Freye, R. K. W. Haselwimmer, and G. G. Lonzarich, *Nature* **394**, 39 (1998).
 - ² H. v. Löhneysen, A. Rosch, M. Vojta, and P. Wölfle, *Rev. Mod. Phys.* **79**, 1015 (2007).
 - ³ P. Gegenwart, Q. Si, and F. Steglich, *Nature Phys.* **4**, 186 (2008).
 - ⁴ S. Nakatsuji, K. Kuga, Y. Machida, T. Tayama, T. Sakakibara, Y. Karaki, H. Ishimoto, S. Yonezawa, Y. Maeno, E. Pearson, G. G. Lonzarich, L. Balicas, H. Lee, and Z. Fisk, *Nature Phys.* **4**, 603 (2008).
 - ⁵ K. Kuga, Y. Karaki, Y. Matsumoto, Y. Machida, and S. Nakatsuji, *Phys. Rev. Lett.* **101**, 137004 (2008).
 - ⁶ Y. Matsumoto, S. Nakatsuji, K. Kuga, Y. Karaki, N. Horie, Y. Shimura, T. Sakakibara, A. H. Nevidomskyy, and P. Coleman, *Science* **331**, 316 (2011).
 - ⁷ M. Okawa, M. Matsunami, K. Ishizaka, R. Eguchi, M. Taguchi, A. Chainani, Y. Takata, M. Yabashi, K. Tamasaku, Y. Nishino, T. Ishikawa, K. Kuga, N. Horie, S. Nakatsuji, and S. Shin, *Phys. Rev. Lett.* **104**, 247201 (2010).
 - ⁸ J. A. Hertz, *Phys. Rev. B* **14**, 1165 (1976).
 - ⁹ T. Moriya, *Spin Fluctuations in Itinerant Electron Magnetism* (Springer, Berlin, 1985).
 - ¹⁰ A. J. Millis, *Phys. Rev. B* **48**, 7183 (1993).
 - ¹¹ Y. Matsumoto, K. Kuga, T. Tomita, Y. Karaki, and S. Nakatsuji, *Phys. Rev. B* **84**, 125126 (2011).
 - ¹² Y. H. Matsuda, T. Nakamura, K. Kuga, S. Nakatsuji, S. Michimura, T. Inami, N. Kawamura, and M. Mizumaki, *J. Korean Phys. Soc.* **62**, 125126 (2013).
 - ¹³ Y. Matsumoto, K. Kentaro, and S. Nakatsuji, *JPS Conf. Proc.* **3**, 011076 (2014).
 - ¹⁴ Y. Matsumoto, K. Kuga, Y. Karaki, T. Tomita, and S. Nakatsuji, *Phys. Status Solidi B* **247**, 720 (2010).
 - ¹⁵ Y. Matsumoto, K. Kuga, N. Horie, and S. Nakatsuji, *J. Phys.: Conf. Ser.* **273**, 012006 (2011).
 - ¹⁶ T. Sakakibara, H. Mitamura, T. Tayama, and H. Amit-suka, *Japan. J. Appl. Phys.* **33**, 5067 (1994).
 - ¹⁷ E. C. T. O'Farrell, Y. Matsumoto, and S. Nakatsuji, *Phys. Rev. Lett.* **109**, 176405 (2012).
 - ¹⁸ Y. Matsumoto, S. Nakatsuji, K. Kuga, Y. Karaki, Y. Shimura, T. Sakakibara, A. H. Nevidomskyy, and P. Coleman, *J. Phys.: Conf. Ser.* **391**, 012041 (2012).
 - ¹⁹ J. H. Pixley, S. Kirchner, K. Ingersent, and Q. Si, *Phys. Rev. Lett.* **109**, 086403 (2012).
 - ²⁰ A. Ramires, P. Coleman, A. H. Nevidomskyy, and A. M. Tsvelik, *Phys. Rev. Lett.* **109**, 176404 (2012).
 - ²¹ A. H. Nevidomskyy and P. Coleman, *Phys. Rev. Lett.* **102**, 077202 (2009).
 - ²² S. Watanabe and K. Miyake, *Phys. Rev. Lett.* **105**, 186403 (2010).
 - ²³ S. Watanabe and K. Miyake, *J. Phys. Soc. Jpn.* **82**, 083704 (2013).
 - ²⁴ K. Deguchi, S. Matsukawa, N. K. Sato, T. Hattori, K. Ishida, H. Takakura, and T. Ishimasa, *Nat. Mater.* **11**, 1013 (2012).
 - ²⁵ S. Watanabe and K. Miyake, *J. Phys. Soc. Jpn.* **83**, 103708 (2014).
 - ²⁶ E. C. T. O'Farrell *et al.*, preprint (2014).
 - ²⁷ M. Bercx and F. F. Assaad, *Phys. Rev. B* **86**, 075108 (2012).
 - ²⁸ Y. Tokiwa, P. Gegenwart, T. Radu, J. Ferstl, G. Sparr, C. Geibel, and F. Steglich, *Phys. Rev. Lett.* **94**, 226402 (2005).
 - ²⁹ P. Gegenwart, Y. Tokiwa, T. Westerkamp, F. Weickert, J. Custers, J. Ferstl, C. Krellner, C. Geibel, P. Kersch, K.-H. Müller, and F. Steglich, *New J. Phys.* **8**, 171 (2006).
 - ³⁰ Y. Tokiwa, P. Gegenwart, F. Weickert, R. Kuchler,

- J. Custers, J. Ferstl, C. Geibel, and F. Steglich, *J. Magn. Mater.* **272-276**, E87 (2004).
- ³¹ P. M. C. Rourke, A. McCollam, G. Lapertot, G. Knebel, J. Flouquet, and S. R. Julian, *Phys. Rev. Lett.* **101**, 237205 (2008).
- ³² H. Pfau, R. Daou, S. Lausberg, H. R. Naren, M. Brando, S. Friedemann, S. Wirth, T. Westerkamp, U. Stockert, P. Gegenwart, C. Krellner, C. Geibel, G. Zwicknagl, and F. Steglich, *Phys. Rev. Lett.* **110**, 256403 (2013).
- ³³ P. Gegenwart, J. Custers, C. Geibel, K. Neumaier, T. Tayama, K. Tenya, O. Trovarelli, and F. Steglich, *Phys. Rev. Lett.* **89**, 056402 (2002).
- ³⁴ S. Nakatsuji, D. Pines, and Z. Fisk, *Phys. Rev. Lett.* **92**, 016401 (2004).